SIAM J. NUMER. ANAL.
Vol. 44, No. 2, pp. 586–612

A MATRIX ANALYSIS OF OPERATOR-BASED UPSCALING FOR THE WAVE EQUATION*

OKSANA KOROSTYSHEVSKAYA† AND SUSAN E. MINKOFF†

Abstract. Scientists and engineers who wish to understand the earth's subsurface are faced with a daunting challenge. Features of interest range from the microscale (centimeters) to the macroscale (hundreds of kilometers). It is unlikely that computational power limitations will ever allow modeling of this level of detail. Numerical upscaling is one technique intended to reduce this computational burden. The operator-based algorithm (developed originally for elliptic flow problems) is modified for the acoustic wave equation. With the wave equation written as a first-order system in space, we solve for pressure and its gradient (acceleration). The upscaling technique relies on decomposing the solution space into coarse and fine components. Operator-based upscaling applied to the acoustic wave equation proceeds in two steps. Step one involves solving for fine-grid features internal to coarse blocks. This stage can be solved quickly via a well-chosen set of coarse-grid boundary conditions. Each coarse problem is solved independently of its neighbors. In step two we augment the coarse-scale problem via this internal subgrid information. Unfortunately, the complexity of the numerical upscaling algorithm has always obscured the physical meaning of the resulting solution. Via a detailed matrix analysis, the coarse-scale acceleration is shown to be the solution of the original constitutive equation with input density field corresponding to an averaged density along coarse block edges. The pressure equation corresponds to the standard acoustic wave equation at nodes internal to coarse blocks. However, along coarse cell boundaries, the upscaled solution solves a modified wave equation which includes a mixed second-derivative term.

Key words. upscaling, multiscale methods, acoustic wave propagation, matrix analysis, seismology

AMS subject classifications. 35L05, 74Q15, 86-08, 86A15, 65M06

DOI. 10.1137/050625369

1. Introduction.

Many problems in physics and engineering result in models involving multiple scales. Often, one is forced to solve partial differential equations with highly oscillatory coefficients over very large spatial domains. The size of the resulting discrete problems makes a direct numerical simulation extremely difficult. In reservoir simulation, for example, it is common to require tens of millions of grid blocks to capture the fluctuations in the permeability of the medium [10]. Upscaling (or multiscale) techniques provide a way to solve the problem on a coarser scale while still capturing some of the effects of the fine scale.

There are two main approaches to upscaling. The first idea involves averaging the input data and thereby forming effective (or upscaled) parameters. A new problem corresponding to this upscaled data is solved on a coarse grid [7], [10]. The second approach allows the problem to be solved on the coarse scale without explicitly forming effective coefficients. Instead, some kind of operator-based technique is used to incorporate the fine-grid information into a coarse solution [4], [14].

Averaging techniques [16], [10] and the methods based on homogenization [7], [8] are examples of the first approach. Averaging is one of the simplest methods for

*Received by the editors February 25, 2005; accepted for publication (in revised form) November 2, 2005; published electronically March 17, 2006. This research was performed with funding from both the Collaborative Math-Geoscience Program at NSF (grant EAR-0222181) and a GAANN grant from the U.S. Department of Education (award P200A030097).

http://www.siam.org/journals/sinum/44-2/62536.html

†Department of Mathematics and Statistics, University of Maryland Baltimore County, 1000 Hilltop Circle, Baltimore, MD 21250 (oksana1@math.umbc.edu, sminkoff@math.umbc.edu).

calculating effective parameters. The general idea is to obtain an effective value on each coarse block as some kind of average (arithmetic, harmonic, or geometric) of the original input parameter field. The averaging methods have a limited range of application. They only give correct results for certain types of media [16].

The methods based on homogenization theory [7], [8], [1] use asymptotic analysis to replace the given problem by a macroscopic problem with simple effective coefficients. (In many cases the effective coefficients are constants.) Homogenization is based on two main hypotheses:

- the medium under study is periodic, and
- the period is small compared to the size of the domain.

In homogenization, the effective parameters are constructed analytically. This construction requires the solution of so-called cell problems—boundary value problems within a single period cell. The main drawback of such methods is that they are, typically, not applicable to realistic nonperiodic structures.

More recently, a number of methods of the second, operator-based, type have been introduced and developed. The multiscale finite element method for elliptic problems with rapidly oscillating coefficients developed by Hou and Wu is an example of this approach [14], [12]. The idea behind the multiscale finite element method is to construct special coarse-scale finite element basis functions which capture the small-scale information within each element. These basis functions are obtained by solving homogeneous elliptic equations in each element subject to specified boundary conditions. The effect of the small scale is then incorporated into the coarse solution through the global stiffness matrix. The main difficulty is that large errors may result from "resonance" between the grid scale and the scales of the continuous problem. An oversampling technique is used to overcome this limitation [9], [18], [13].

Another example of the operator-based approach to upscaling is the mortar method [15], [19]. This method is based on domain decomposition. The physical domain is decomposed into a series of blocks in which different numerical grids, physical models, and discretization techniques can be used. Mortar finite element spaces are then used to allow for nonmatching grids across the block interfaces and to impose physically meaningful interface continuity conditions. One of the advantages of the method is that one may vary the number of mortar degrees of freedom and thus achieve improvements in accuracy. The disadvantage of the mortar technique is that it can be expensive, especially when a large number of degrees of freedom are used in the interface problems.

The operator-based upscaling technique was introduced for elliptic equations by Arbogast, Minkoff, and Keenan in [4]. The method was further developed by Arbogast et al. in [3], [6], [5]. The idea of the method is to decompose the solution into two parts: a coarse grid representation and a subgrid component. The subgrids are the portions of the domain contained within each of the coarse-grid cells. The problem is solved in two steps. First, we solve for the fine-scale information internal to each coarse cell. Due to a simplifying assumption imposed on the boundaries of the coarse cells, these subgrid problems decouple and can be solved independently. The second step involves using the subgrid solutions to modify the coarse-scale operator. The resulting coarse-scale solution includes some of the fine-scale features of the problem under study. A significant advantage of this method is that we use data provided on the fine scale directly in our computations (no averaging). Further, we need not assume that the medium is periodic. Perhaps most importantly, however, the operator upscaling method does not assume a separation of scales (a fundamental underlying assumption of asymptotic techniques). Geologic materials contain heterogeneities on

a continuum of scales which for realistic problems negates the basic separation of scales hypothesis.

In the companion paper by Vdovina, Minkoff, and Korostyshevskaya [17] we adapt operator-based upscaling for use with the acoustic wave equation. We focus on the second-order in space and time acoustic wave equation which we write as a system of two first-order equations (in space). Thus we solve for both pressure and its derivative (acceleration). The practical details of both the serial and parallel implementations of the algorithm are described in that paper. Specifically we detail the numerical implementation of the system described in section 2.1 of this paper (the original upscaled system). The two-stage algorithm requires solving the subgrid equations (2.5–2.6) and the coarse equation (2.7) for each time step. In Vdovina et al. [17] we describe the relative costs of the serial and parallel implementations as well. Upscaling by definition implies that we are not solving the full fine-grid problem. Some simplifications must be made to speed up the computation. With this method our primary simplification is that we impose zero flux conditions between coarse blocks at the subgrid stage of the algorithm (when we solve for internal subwavelength scale information). This assumption means that the most costly part of the algorithm (the subgrid solve) is trivial to parallelize. Each coarse cell is solved independently of its neighbors. Thus we achieve near-optimal speedup for the parallel upscaling algorithm. Because acceleration is upscaled but pressure is defined only on the fine grid in our current implementation, we find that standard fine grid stability and dispersion results (CFL and number of gridpoints per wavelength) hold. (Extensions of the method for upscaling both pressure and acceleration are also discussed in [17].) Finally, three realistic numerical experiments are described in that paper. We compare the upscaled solution to a full finite difference solution of the wave equation for a periodic (checkerboard) velocity, a finely layered medium, and a stochastic velocity field describing a two-component mixture of materials taken from a von Karman distribution. These three velocity fields were chosen primarily for their geologic relevance. (They contain basic components one might encounter in subsurface regions such as the Gulf of Mexico or deep crust.) The upscaled solution qualitatively captures even the subwavelength-scale heterogeneity of the full solution.

Our focus in this work is on addressing the question of what the upscaled solution means. What physics does the solution model? Is our model still the acoustic wave equation or an attenuated version of the wave equation? We provide the first answers to these questions in this paper via a linear algebra analysis of the method. What this analysis highlights is that the numerical upscaling process solves a constitutive equation similar in form to the original equation. The constitutive equation relates acceleration to the gradient of pressure. For the coarse (upscaled) problem, however, the parameter field (density) reduces to an averaged density along coarse block edges. Similarly, when analyzing the pressure equation, we find the upscaled solution solves the original wave equation at nodes internal to the coarse blocks, but a modified equation at coarse block edges. Specifically, a cross-derivative (involving differentiation with respect to both x and y) enters the standard wave equation. This analysis not only simplifies the coding of the algorithm but illuminates the physical meaning of the upscaled solution. In this paper, we focus on the theory. (We do not include numerical experiments based on the system of equations which result from the analysis given in this paper.) However, the new formulation should simplify the simulations described in [17] considerably and is the subject of future work. The standard implementation of operator upscaling involves technicalities (such as the use of numerical Green's functions) that are no longer necessary as a result of this analysis.

It is important to point out that the equations which result from this analysis (specifically the conclusions of Theorems 1, 10, and 11) are to our knowledge entirely new. While other papers exist which discuss convergence of operator upscaling for elliptic problems in the context of finite elements, no other work (outside this paper and the related work by Vdovina et al. [17]) discusses operator upscaling for the wave equation. More importantly, the physics modeled by operator upscaling has not been illuminated (for any PDE) prior to this work.

In the remainder of the paper we describe the mathematics behind the upscaling algorithm. Then we begin the matrix analysis of the two-equation system. First we analyze the constitutive equation for coarse acceleration. The result is both a finite difference stencil and a continuous differential equation corresponding to the upscaled acceleration equation. Finally, we apply a similar analysis to the pressure equation. We define the finite difference stencils for pressure (which depend on the location of the pressure unknown within the coarse block) and corresponding continuous differential equations coming from the upscaling algorithm.

2. Upscaled acoustic wave equation.

2.1. Subgrid upscaling for the acoustic wave equation: Variational formulation. Let Ω be a two-dimensional domain with boundary Γ. We consider the acoustic wave equation in Ω written as a first-order system for acceleration $\vec{v}$ and pressure p:

$$\vec{v} = -\frac{1}{\rho}\nabla p, \tag{2.1}$$

$$\frac{1}{\rho c^2}\frac{\partial^2 p}{\partial t^2} = -\nabla \cdot \vec{v} + f. \tag{2.2}$$

Here c is the sound velocity, ρ is the density, and f is the source of acoustic energy. Both c and ρ are functions of spatial location only *and are assumed to be heterogeneous.* To simplify the presentation of the method, we will assume zero boundary conditions:

$$\vec{v} \cdot \vec{\nu} = 0 \quad \text{on} \quad \Gamma,$$

where $\vec{\nu}$ is the unit outward normal vector.

The subgrid upscaling technique is developed in the context of a mixed finite element method. Let

$$H_0(\text{div}, \Omega) = \{\vec{v} \in (L^2(\Omega))^2 : \nabla \cdot \vec{v} \in L^2(\Omega), \text{ and } \vec{v} \cdot \vec{\nu} = 0 \text{ on } \Gamma\}.$$

We rewrite (2.1)–(2.2) in weak form as follows: find $\vec{v} \in H_0(\text{div}; \Omega)$ and $p \in L^2(\Omega)$ such that

$$\langle \rho \vec{v}, \vec{u} \rangle = \langle p, \nabla \cdot \vec{u} \rangle \,, \tag{2.3}$$

$$\left\langle \frac{1}{\rho c^2}\frac{\partial^2 p}{\partial t^2}, w \right\rangle = -\langle \nabla \cdot \vec{v}, w \rangle + \langle f, w \rangle \tag{2.4}$$

for all $\vec{u} \in H_0(\text{div}; \Omega)$ and $w \in L^2(\Omega)$.

The idea of the upscaling method is that while the original problem is posed on a fine grid (specifically the input acceleration and density are measured fields on the fine grid), our goal is to solve the problem on a coarse mesh. We wish to capture some of the fine-scale information internal to each coarse cell and then to use this

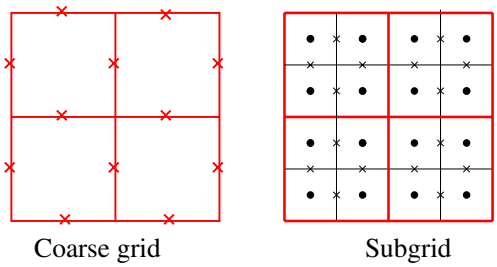

FIG. 2.1. *A 2×2 coarse grid with coarse acceleration unknowns and a corresponding 4×4 fine grid with subgrid unknowns. Pressures live at the centers of the cells. Acceleration lives on cell edges.*

information to determine the best solution possible on the coarse scale. We break the acceleration into two parts—the coarse representation (coarse-grid unknowns) and the subgrid part (fine-grid unknowns internal to each coarse-grid cell):

$$\vec{v} = \vec{v}^c + \delta\vec{v}.$$

In earlier work the pressure space was also decomposed. (See [4] for an example of this decomposition for the elliptic pressure equation.) Unfortunately, the basis functions for the pressure space are computationally clumsy. Since no additional work is required to keep the pressure on the fine grid, we have chosen to only decompose acceleration in this paper. Pressure can be projected onto the coarse grid as a post-processing step if so desired.

In the mixed finite element method, we use a rectangular two-scale mesh and approximate the pressure and the acceleration in finite element spaces W and V, respectively. We take the pressure space W to be the space of piecewise discontinuous constant functions on the fine grid with nodes at the centers of the cells. To define the acceleration space V for the upscaling method, we introduce two finite element spaces δV and V^c associated with the fine and coarse computational grids. Both of these spaces consist of piecewise linear vector functions of the form (a_1x+b_1, a_2y+b_2) living on the edges of the grid blocks (see Figure 2.1). We impose an important simplifying condition on the space δV, namely,

$$\delta\vec{u} \cdot \vec{\nu} = 0 \quad \text{on the boundary of each coarse element.}$$

This is the only simplifying assumption in the definition of our method. It allows us to decouple the subgrid problems coming from different coarse-grid cells. Note that this simplifying assumption only applies to the solution of the subgrid problems which were never intended to be solved exactly but merely approximated. Exact solution of the subgrid problems would lead us back to a full finite difference solution of the wave equation.

The upscaling process consists of two steps. First, we restrict to the subgrid test functions in (2.3)–(2.4) and use the above decomposition to obtain a series of subgrid problems, one for each coarse element E_c:

$$\langle \rho(\vec{v}^c + \delta\vec{v}), \delta\vec{u}\rangle = \langle p, \nabla \cdot \delta\vec{u}\rangle, \tag{2.5}$$

$$\left\langle \frac{1}{\rho c^2}\frac{\partial^2 p}{\partial t^2}, w \right\rangle = -\langle \nabla \cdot (\vec{v}^c + \delta\vec{v}), w\rangle + \langle f, w\rangle \tag{2.6}$$

for all $\delta\vec{u} \in \delta V$, $w \in W$. The values of $\vec{v}^c$ are unknown at this stage, so we find the solution to the subgrid problem as a function of the coarse unknowns. Note, that the pressure is completely determined by (2.5–2.6).

The second step of the upscaling process uses $\delta\vec{v}$ and p to determine $\vec{v}^c \in V^c$ through solution of the upscaled coarse equation ((2.3) with coarse-grid test functions):

$$\langle \rho(\vec{v}^c + \delta\vec{v}(\vec{v}^c)), \vec{u}^c \rangle = \langle p, \nabla \cdot \vec{u}^c \rangle \tag{2.7}$$

for all $\vec{u}^c \in V^c$.

The problem is solved sequentially in time. We use second-order finite differences to approximate the time derivative in (2.6). First, we find the pressure on the current time level using the velocities and pressure from the previous time levels. Then we solve (2.5) and (2.7) for the subgrid and coarse velocities. The process then repeats for the next time step.

2.2. A matrix analysis discussion of subgrid upscaling. One of the main purposes of this paper is to derive the explicit coarse-scale equation solved by the upscaling algorithm using the discrete form of the subgrid and coarse problems. The advantage of using the discrete formulation is that it allows us to obtain both finite difference and continuous differential equations for coarse acceleration. The finite difference equation yields an explicit stencil for pressure and coarse acceleration that could be implemented directly, thus giving an alternate, simpler way to code the algorithm over that which is detailed in section 2.1 of this paper and in [17]. This analysis shows that coarse acceleration is defined using the average of density values on the boundaries of coarse cells (in a sense defining an upscaled density). From the finite difference equation we can derive the continuous differential equation for the coarse problem which is similar to the original equation (2.1) with density replaced by the upscaled density. We see that the upscaled acceleration approximates the gradient of pressure on the *boundaries* of the coarse cells compensating for the simplifying zero boundary conditions used by the algorithm. In this section, we derive the matrix-vector form of the subgrid and coarse problems. In terms of linear algebra, we see that the subgrid problems can easily be solved for the subgrid acceleration in terms of the pressure and the coarse acceleration. Thus, we can eliminate the subgrid unknowns from the coarse problem to obtain a matrix equation for the coarse acceleration and pressure only. The analysis of the resulting system allows us to determine the differential equation solved by the upscaling algorithm and to understand the physical meaning of the coarse part of the solution.

Homogenization is an alternate technique for analyzing equations with parameters and unknowns that contain multiple scales. The operator upscaling analysis given in this paper is complete in itself and is distinct from a homogenization analysis. Future work may include comparison of operator-based upscaling results to those obtained from asymptotic series solutions. Arbogast and Boyd [2] examine the connection between the multiscale finite element method (a numerical technique based on homogenization) and operator upscaling in the context of elliptic problems. We do not discuss connections between methods here.

We begin by describing the finite element context in which the method is developed. In order to discretize the subgrid and the coarse problems, we use finite element approximations of the unknown functions. In this paper, we restrict our attention to the x component v_x of the acceleration vector, since the equations for v_y are similar.

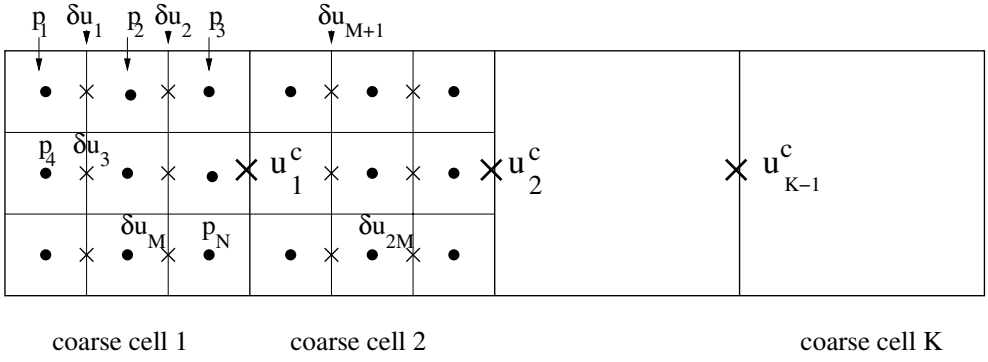

FIG. 2.2. *Subgrid and coarse unknowns. The grid consists of K total coarse cells.*

To simplify notation, consider a domain consisting of one row of coarse cells, each subdivided into a number of fine cells (Figure 2.2). If K is the number of coarse cells, we divide each coarse cell into n_x fine cells in the x direction and n_y fine cells in the y direction. Then the number of fine cells in one coarse block is $N = n_x n_y$, and the total number of fine cells is KN.

In the subgrid upscaling method we will describe here, both the coarse and fine components of the horizontal acceleration are approximated by the space of piecewise continuous linear functions in x and piecewise constants in y. Obviously, other choices of finite element spaces are also possible. However, this choice is the simplest. The coarse and subgrid basis functions $(u_x^c)_i$, $(\delta u_x)_i$ for the acceleration space have nodes at the midpoints of vertical edges of the coarse cells for the coarse acceleration and at the midpoints of vertical edges of the fine cells for the subgrid acceleration (Figure 2.2). At time t,

$$v_x^c(t,x,y) = \sum_{i=1}^{K-1} (\mathbf{v_x^c})_i(t)(u_x^c)_i(x,y), \tag{2.8}$$

$$\delta v_x(t,x,y) = \sum_{i=1}^{MK} (\delta \mathbf{v_x})_i(t)(\delta u_x)_i(x,y). \tag{2.9}$$

Here, $K-1$ is the number of the coarse acceleration unknowns, M is the number of the subgrid acceleration unknowns inside one coarse cell so that MK is the total number of the subgrid acceleration unknowns in the domain, and the coefficients $(\mathbf{v_x^c})_i$, $(\delta \mathbf{v_x})_i$ are to be determined. Since the subgrid acceleration lives on the vertical edges of the fine cells and there are no nodes on the boundaries of the coarse cells, we have that $M = N - n_y$.

The pressure p is approximated by piecewise constants defined on the fine grid. Thus, we have the expansion

$$p(t,x,y) = \sum_{i=1}^{NK} \mathbf{p}_i(t) w_i(x,y). \tag{2.10}$$

Here NK is the total number of pressure unknowns, and w_m is the basis function for pressure, which takes the value 1 on the mth subgrid cell and 0 everywhere else.

We will now derive the matrix forms of the subgrid and coarse problems and then use these equations to eliminate the subgrid unknowns from the coarse problem. To

obtain a linear system from subgrid equations (2.5)–(2.6), we use the finite element expansions given in (2.8)–(2.10):

(2.11)
$$\sum_{j=1}^{K-1}(\mathbf{v_x^c})_j\langle\rho(u_x^c)_j,(\delta u_x)_i\rangle+\sum_{j=1}^{MK}(\delta\mathbf{v_x})_j\langle\rho(\delta u_x)_j,(\delta u_x)_i\rangle=\sum_{j=1}^{NK}\mathbf{p}_j\left\langle w_j,\frac{\partial(\delta u_x)_i}{\partial x}\right\rangle,\quad i=1,2,\ldots,MK,$$

and

(2.12)
$$\sum_{j=1}^{NK}\frac{\partial^2\mathbf{p}_j}{\partial t^2}\left\langle\frac{1}{\rho c^2}w_j,w_i\right\rangle=-\sum_{j=1}^{K-1}(\mathbf{v_x^c})_j\left\langle\frac{\partial(u_x^c)_j}{\partial x},w_i\right\rangle-\sum_{j=1}^{MK}(\delta\mathbf{v_x})_j\left\langle\frac{\partial(\delta u_x)_j}{\partial x},w_i\right\rangle-(v_y\text{ terms})+\langle f,w_i\rangle,\quad i=1,2,\ldots,NK.$$

These equations can be written in matrix form by defining the following matrix entries:

$$a_{i,j}^{ff}=\langle\rho(\delta u_x)_j,(\delta u_x)_i\rangle,\quad a_{i,j}^{cf}=\langle\rho(u_x^c)_j,(\delta u_x)_i\rangle,\quad b_{i,j}^{f}=\left\langle w_j,\frac{\partial(\delta u_x)_i}{\partial x}\right\rangle,\tag{2.13}$$

$$w_{i,j}=\left\langle\frac{1}{\rho c^2}w_j,w_i\right\rangle,\qquad f_i=\langle f,w_i\rangle,\qquad b_{i,j}^{c}=\left\langle w_j,\frac{\partial(u_x^c)_i}{\partial x}\right\rangle.\tag{2.14}$$

Then the subgrid system reduces to the following linear system:

$$A^{cf}\mathbf{v_x^c}+A^{ff}\delta\mathbf{v_x}=B^f\mathbf{p},\tag{2.15}$$

$$W\frac{\partial^2\mathbf{p}}{\partial t^2}=-(B^c)^T\mathbf{v_x^c}-(B^f)^T\delta\mathbf{v_x}-(v_y\text{ terms})+F.\tag{2.16}$$

Similar steps lead to a discretization of the coarse problem (2.7). We obtain the matrix equation:

$$A^{cc}\mathbf{v_x^c}+(A^{cf})^T\delta\mathbf{v_x}=B^c\mathbf{p},\tag{2.17}$$

where the matrix A^{cc} has entries

$$a_{i,j}^{cc}=\langle\rho(u_x^c)_j,(u_x^c)_i\rangle.\tag{2.18}$$

We will now use the matrix form of the subgrid and coarse problems to eliminate the subgrid unknowns from the coarse equation. The subgrid equations are coupled to the coarse scale unknowns. In particular, (2.15) involves coarse acceleration unknowns $\mathbf{v_x^c}$, which are not known at the subgrid step of the algorithm. This equation can easily be solved for $\delta\mathbf{v_x}$ in terms of $\mathbf{v_x^c}$

$$\delta\mathbf{v_x}=-(A^{ff})^{-1}A^{cf}\mathbf{v_x^c}+(A^{ff})^{-1}B^f\mathbf{p}.\tag{2.19}$$

Substituting (2.19) into the coarse problem (2.17), we obtain the matrix equation for the coarse acceleration and pressure only,

$$(A^{cc}-(A^{cf})^T(A^{ff})^{-1}A^{cf})\mathbf{v_x^c}=(B^c-(A^{cf})^T(A^{ff})^{-1}B^f)\mathbf{p}\tag{2.20}$$

or

$$U\mathbf{v}_{\mathbf{x}}^{\mathbf{c}} = D\mathbf{p}. \tag{2.21}$$

Formula (2.21) gives us the matrix equation for the coarse acceleration and pressure. We will use (2.21) later to derive a difference and then differential equations for the coarse acceleration. Therefore, it is worthwhile to study the structure of the matrices U and D, and to explicitly define their entries. In Theorem 1, we show that the choice of bases for the finite element spaces results in matrices which are sparse and have special structure. Moreover, we obtain simple explicit formulas for the entries by computing them with special quadrature rules defined on the fine grid. The choice to use fine grid quadratures is based on the assumption that the parameter fields ρ and c vary on the fine scale. We do not want to introduce averaging errors by requiring these parameters to live on the coarse grid.

Let us begin with some notation that will be used throughout the rest of this paper. Let h_x and h_y be the lengths of a single fine cell in the x and y directions respectively, and H_x, H_y the lengths of a single coarse cell in these two directions. We denote by ρ_l and $(u_x^c)_j|_l$ the values of the density and coarse acceleration basis functions at the lth node of subgrid acceleration, and by ρ_l^j the values of the density on the boundary of the coarse cell corresponding to the jth coarse acceleration node.

THEOREM 1. *Consider the set of subgrid problems* (2.5)–(2.6) *and the coarse problem* (2.7). *The upscaling technique results in the linear system for the coarse acceleration and pressure of the form*

$$U\mathbf{v}_{\mathbf{x}}^{\mathbf{c}} = D\mathbf{p},$$

where U and D are given by (2.20)–(2.21). *U is of size $(K-1)\times(K-1)$ and D is of size $(K-1)\times NK$.*

Further, assume the density ρ and sound velocity c are smooth enough for the inner products in the matrix entries U and D to be computed using fine-grid midpoint and trapezoidal rules. Then the matrix U is diagonal and the matrix D is block upper bidiagonal with blocks of size $1\times N$. The entries of U are given by the sum of density values on the corresponding boundaries of the coarse cells

$$U_{i,i} = (h_x h_y)\sum_{l=1}^{n_y}\rho_l^i. \tag{2.22}$$

The blocks of D are given by

$$D_{i,i} = \frac{h_x h_y}{h_x}\left[0,\quad 0,\quad \ldots,\quad 1,\quad \ldots,\quad 0,\quad 0,\quad \ldots\quad 1\right], \tag{2.23}$$

$$D_{i,i+1} = \frac{h_x h_y}{h_x}\left[-1,\quad 0,\quad \ldots,\quad 0,\quad \ldots,\quad -1,\quad 0,\quad \ldots,\quad 0\right], \tag{2.24}$$

where the nonzero entries correspond to the pressure nodes located along the boundaries of the coarse cells.

Note. In this Theorem, we are using the trapezoidal rule on the fine grid in the x direction and the midpoint rule in the y direction to compute the integrals. When these rules are used, the quadrature node points coincide with the nodes of the subgrid basis functions. This fact simplifies the formulas for the matrix entries. Even more

importantly, both the midpoint rule and the trapezoidal rule are accurate enough that no additional error is incurred for our choice of interpolating polynomials.

The results of Theorem 1 will allow us to determine the explicit difference equation for coarse acceleration solved by the upscaling algorithm and to understand the physical meaning of the resulting problem solution.

Proof. First, let us discuss the coefficient matrix U of coarse acceleration. Recall that

$$U = A^{cc} - (A^{cf})^T (A^{ff})^{-1} A^{cf}. \tag{2.25}$$

In order to explicitly define the entries of U, we need to study the matrices A^{cc}, A^{cf}, and A^{ff}. The following lemmas describe the structure of these matrices.

LEMMA 2. *The matrix A^{cf} is a lower bidiagonal $K \times (K-1)$ block matrix with blocks of size $M \times 1$. If the entries of the matrix are evaluated by the trapezoidal rule in x and the midpoint rule in y on each fine cell, then*

$$a^{cf}_{l,j} = (h_x h_y) \rho_l (u^c_x)_j|_l. \tag{2.26}$$

Proof. The entries of the matrix A^{cf} are the inner products of the coarse and subgrid acceleration basis functions (2.13). Since the total number of subgrid acceleration basis functions is MK and the total number of coarse acceleration basis functions is $K-1$, the matrix A^{cf} is of size $MK \times (K-1)$.

Each coarse acceleration basis function is supported on two coarse cells and, therefore, has nonzero inner products with the subgrid functions from these coarse cells only. For example, the first coarse acceleration basis function is nonzero on the coarse cells 1 and 2 (Figure 2.2). Thus we can partition the matrix into blocks of size $M \times 1$ (where M is the number of subgrid acceleration nodes inside a single coarse cell). Each block A^{cf}_{ij} represents the interaction of the jth coarse basis function with the ith coarse cell. Then the matrix A^{cf} can be written as a $K \times (K-1)$ lower bidiagonal block matrix:

$$A^{cf} = \begin{bmatrix} A^{cf}_{1,1} & & & 0 \\ A^{cf}_{2,1} & A^{cf}_{2,2} & & \\ & \ddots & \ddots & \\ & & & A^{cf}_{K-1,K-1} \\ 0 & & & A^{cf}_{K,K-1} \end{bmatrix}. \tag{2.27}$$

We can evaluate the matrix entries by the trapezoidal rule in x and the midpoint rule in y on each fine cell, so that the quadrature nodal points coincide with the fine acceleration nodes (Figure 2.3). Applying these rules to each entry gives a product of the area of the cell $(h_x h_y)$ with the value of the integrand at the nodal points of the fine acceleration. Since any subgrid acceleration basis function is 1 at the corresponding node and 0 at all other nodes, we obtain

$$a^{cf}_{l,j} = \langle \rho (u^c_x)_j, (\delta u_x)_l \rangle = (h_x h_y) \rho_l (u^c_x)_j \big|_l. \qquad \square$$

LEMMA 3. *If the entries of the matrix A^{ff} are evaluated by the trapezoidal rule in x and the midpoint rule in y on each fine cell, then A^{ff} is an $MK \times MK$ diagonal matrix with entries*

$$a^{ff}_{ll} = (h_x h_y) \rho_l.$$

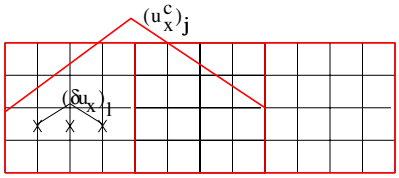

FIG. 2.3. *Coarse and subgrid acceleration basis functions* $(u_x^c)_j$ *and* $(\delta u_x)_l$. *The crosses represent the subgrid acceleration nodes which are used as quadrature nodal points.*

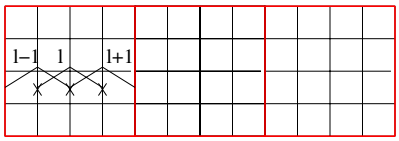

FIG. 2.4. *Subgrid acceleration basis functions* $(\delta u_x)_{l-1}$, $(\delta u_x)_l$, *and* $(\delta u_x)_{l+1}$. *The crosses represent the subgrid acceleration nodes which are used as quadrature nodal points.*

Note. A^{ff} is the coefficient matrix of subgrid unknowns in (2.15). The fact that we are able to reduce A^{ff} to a diagonal matrix makes the elimination of the subgrid unknowns cheap and easy.

Proof. The matrix A^{ff} is the coefficient matrix of subgrid unknowns in (2.15) and its entries are the inner products of subgrid acceleration basis functions (2.13). The total number of subgrid acceleration basis functions is MK, so the matrix A^{ff} has size $MK \times MK$. Each subgrid acceleration basis function interacts with itself and its neighbors to the left and to the right. As in Lemma 2, we use the trapezoidal rule in x and the midpoint rule in y on each fine cell to compute the entries. The quadrature nodal points coincide with the fine acceleration nodes (Figure 2.4). We obtain

$$a^{ff}_{l,l+1} = \langle \rho(\delta u_x)_l, (\delta u_x)_{l+1} \rangle = 0, \qquad a^{ff}_{l-1,l} = \langle \rho(\delta u_x)_{l-1}, (\delta u_x)_l \rangle = 0, \tag{2.28}$$

$$a^{ff}_{l,l} = \langle \rho(\delta u_x)_l, (\delta u_x)_l \rangle = (h_x h_y)\rho_l. \tag{2.29}$$

Here, we made use of the fact that any subgrid acceleration basis function is 1 at the corresponding node and 0 at all other nodes. We see that if the entries are computed as above, the matrix A^{ff} is diagonal. ∎

LEMMA 4. *The matrix* A^{cc} *is a* $(K-1)\times(K-1)$ *tridiagonal matrix. If the entries of* A^{cc} *are evaluated by the composite trapezoidal rule in the* x *direction and the midpoint rule in the* y *direction, then*

$$a^{cc}_{j,j+1} = (h_x h_y) \sum_{l=Mj+1}^{M(j+1)} \rho_l (u_x^c)_{j+1} (u_x^c)_j \big|_l,$$

$$a^{cc}_{j,j-1} = (h_x h_y) \sum_{l=M(j-1)+1}^{Mj} \rho_l (u_x^c)_{j-1} (u_x^c)_j \big|_l,$$

$$a^{cc}_{j,j} = (h_x h_y) \sum_{l=M(j-1)+1}^{M(j+1)} \rho_l (u_x^c)_j^2 \big|_l + (h_x h_y) \sum_{l=1}^{n_y} \rho_l^j.$$

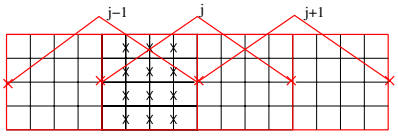

FIG. 2.5. *Coarse acceleration basis functions* $(u_x^c)_{j-1}$, $(u_x^c)_j$, *and* $(u_x^c)_{j+1}$. *The crosses represent the subgrid acceleration nodes* $l = M(j-1)+1, \dots Mj$, *which are used as quadrature nodal points in the computation of* $a^{cc}_{j,j-1}$.

Proof. The entries of the matrix A^{cc} are the inner products of coarse acceleration basis functions (2.18). The total number of the coarse acceleration nodes in the domain is $K-1$, therefore, the matrix has size $(K-1)\times(K-1)$.

Since each coarse acceleration basis function is supported on two coarse cells and interacts with both its neighbors (Figure 2.5), the matrix A^{cc} is tridiagonal. The entries can be computed by the composite trapezoidal rule in the x direction and composite midpoint rule in y on each coarse cell so that the quadrature nodal points coincide with the fine acceleration nodes. Fine grid quadrature is used because the parameter fields ρ and c live on the fine grid, and we do not want to average these parameters. We obtain

$$a^{cc}_{j,j-1} = \langle \rho(u_x^c)_{j-1}, (u_x^c)_j \rangle = (h_x h_y) \sum_{l=M(j-1)+1}^{Mj} \rho_l (u_x^c)_{j-1}\big|_l (u_x^c)_j\big|_l, \tag{2.30}$$

where M is the number of subgrid acceleration nodes inside one coarse cell, and the indices $M(j-1)+1,\dots,Mj$ represent the subgrid acceleration nodes inside coarse cell j (Figure 2.5). Notice that only the nodes internal to the coarse cell are involved in the computation, since either $(u_x^c)_j$ or $(u_x^c)_{j-1}$ is zero on its boundary. Similarly, for $\langle \rho(u_x^c)_{j+1}, (u_x^c)_j \rangle$ we have

$$a^{cc}_{j,j+1} = \langle \rho(u_x^c)_{j+1}, (u_x^c)_j \rangle = (h_x h_y) \sum_{l=Mj+1}^{M(j+1)} \rho_l (u_x^c)_{j+1}\big|_l (u_x^c)_j\big|_l, \tag{2.31}$$

where we sum over the subgrid acceleration nodes inside coarse cell $j+1$. The entry $\langle \rho(u_x^c)_j, (u_x^c)_j \rangle$ is the inner product of the coarse basis function with itself and, therefore, is supported on two coarse cells. We compute the diagonal entry using the composite trapezoidal rule in x and midpoint in y

$$a^{cc}_{j,j} = \langle \rho(u_x^c)_j, (u_x^c)_j \rangle = (h_x h_y) \sum_{l=M(j-1)+1}^{M(j+1)} \rho_l (u_x^c)_j^2\big|_l + (h_x h_y) \sum_{l=1}^{n_y} \rho_l^j. \tag{2.32}$$

The indices $M(j-1)+1,\dots,M(j+1)$ in the first term represent the subgrid acceleration nodes inside coarse cells j and $j+1$. The last term on the right corresponds to the boundary between the two cells at which the basis function $(u_x^c)_i$ has value 1, and ρ_l^j are the values of the density on this boundary. ∎

Proof of formula (2.22) *for* U. Let us now use the above results to study the matrix $U = A^{cc} - (A^{cf})^T (A^{ff})^{-1} A^{cf}$, the coefficient matrix of coarse acceleration in (2.21). Performing block matrix multiplications in $(A^{cf})^T (A^{ff})^{-1} A^{cf}$ and using Lemmas 2 and 3, we see that the product $(A^{cf})^T (A^{ff})^{-1} A^{cf}$ is a tridiagonal matrix.

Let us derive a formula for its upper diagonal entries. For convenience of notation, we present the derivation of the first upper diagonal entry $[(A^{cf})^T(A^{ff})^{-1}A^{cf}]_{1,2}$. The derivation of the rest of the entries is similar. We use the block notation for A^{cf} introduced in Lemma 2 and the fact that A^{ff} is diagonal (Lemma 3) to obtain

$$[(A^{cf})^T(A^{ff})^{-1}A^{cf}]_{1,2} = (A^{cf}_{2,1})^T \begin{bmatrix} (a^{ff}_{M+1,M+1})^{-1} & \dots & 0 \\ \vdots & & \\ 0 & \dots & (a^{ff}_{2M,2M})^{-1} \end{bmatrix} A^{cf}_{2,2}, \tag{2.33}$$

where the blocks $A^{cf}_{2,2}$ and $(A^{cf}_{2,1})^T$ have size $M \times 1$ and $1 \times M$, respectively. The block $A^{cf}_{2,1}$ represents the interaction of the first coarse acceleration basis function $(u^c_x)_1$ with the subgrid acceleration basis functions from the second coarse cell. The explicit formula (2.26) for the entries of A^{cf} gives that

$$(A^{cf}_{2,1})^T = (h_x h_y) \left[\rho_{M+1}(u^c_x)_1\big|_{M+1} \quad \dots \quad \rho_{2M}(u^c_x)_1\big|_{2M} \right], \tag{2.34}$$

where the indices $M+1, \dots, 2M$ are the subgrid acceleration nodes inside the second coarse cell (Figure 2.2). Similarly, the block $A^{cf}_{2,2}$ consists of the inner products of the second coarse acceleration basis function $(u^c_x)_2$ with the subgrid basis functions from the second coarse cell and is given by

$$A^{cf}_{2,2} = (h_x h_y) \begin{bmatrix} \rho_{M+1}(u^c_x)_2\big|_{M+1} \\ \vdots \\ \rho_{2M}(u^c_x)_2\big|_{2M} \end{bmatrix}. \tag{2.35}$$

The explicit formula (2.29) for the entries of A^{ff} and (2.34)–(2.35) result in

$$[(A^{cf})^T(A^{ff})^{-1}A^{cf}]_{1,2} = (h_x h_y) \sum_{l=M+1}^{2M} \rho_l (u^c_x)_2\big|_l (u^c_x)_1\big|_l. \tag{2.36}$$

We can obtain a general formula for the $(j, j+1)$-upper diagonal entry:

$$[(A^{cf})^T(A^{ff})^{-1}A^{cf}]_{j,j+1} = (h_x h_y) \sum_{l=Mj+1}^{M(j+1)} \rho_l (u^c_x)_{j+1}\big|_l (u^c_x)_j\big|_l. \tag{2.37}$$

Following the same manipulations, we derive the lower diagonal and diagonal entries

$$[(A^{cf})^T(A^{ff})^{-1}A^{cf}]_{j,j-1} = (h_x h_y) \sum_{l=M(j-1)+1}^{Mj} \rho_l (u^c_x)_{j-1}\big|_l (u^c_x)_j\big|_l, \tag{2.38}$$

$$[(A^{cf})^T(A^{ff})^{-1}A^{cf}]_{j,j} = (h_x h_y) \sum_{l=M(j-1)+1}^{M(j+1)} \rho_l (u^c_x)^2_j\big|_l. \tag{2.39}$$

Thus, summing the result for entries of A^{cc} from Lemma 4 ((2.30)–(2.32)) with results (2.37)–(2.39) gives us explicit formulas for the entries of U:

$$U_{j,j+1} = 0, \qquad U_{j,j-1} = 0, \qquad U_{j,j} = (h_x h_y) \sum_{l=1}^{n_y} \rho_l^j. \tag{2.40}$$

We see that the matrix U is diagonal and its entries depend only on those values of density which lie on the corresponding boundary of the coarse cell. ∎

Now let us turn our attention to the coefficient matrix of pressure, namely, D. This matrix is defined by

$$D = B^c - (A^{cf})^T (A^{ff})^{-1} B^f. \tag{2.41}$$

In order to write explicit formulas for the entries of D, we need to study the matrices A^{cf}, A^{ff}, B^f, and B^c. We have already discussed the matrices A^{cf} and A^{ff}. The following two lemmas describe the structure of the matrices B^c and B^f.

LEMMA 5. *The matrix B^f is a block diagonal $Kn_y \times Kn_y$ matrix with blocks of size $(n_x - 1) \times n_x$. The blocks of the matrix are given by*

$$T = -\frac{h_x h_y}{h_x} \begin{bmatrix} -1 & 1 & 0 & \dots & 0 & 0 \\ 0 & -1 & 1 & \dots & 0 & 0 \\ & \dots & \dots & & & \\ 0 & 0 & 0 & \dots & -1 & 1 \end{bmatrix}. \tag{2.42}$$

Proof. The entries of the matrix B^f are the inner products of the x derivative of subgrid acceleration basis functions with pressure basis functions, $b^f_{l,m} = \langle w_m, \frac{\partial(\delta u_x)_l}{\partial x} \rangle$. Since the total number of subgrid acceleration basis functions is $Kn_y(n_x - 1)$ and the total number of pressure basis functions is $Kn_y n_x$, the matrix B^f is of size $Kn_y(n_x - 1) \times Kn_y n_x$. The entries of the matrix can be evaluated easily since the subgrid acceleration basis function is piecewise linear in x and constant in y, so its derivative is easily computed

$$\frac{\partial(\delta u_x)_l}{\partial x} = \begin{cases} \dfrac{1}{h_x} & \text{left branch,} \\ -\dfrac{1}{h_x} & \text{right branch.} \end{cases} \tag{2.43}$$

Then $b^f_{l,m} = \pm(h_x h_y)\frac{1}{h_x}$ whenever the pressure basis function and the subgrid acceleration basis function have the same support. Since each subgrid acceleration basis function interacts with only two pressure nodes, one block of the matrix B^f has the form (2.42). Each block corresponds to the interactions of one row of the pressure and acceleration basis functions within a single coarse cell. Since one row of fine cells inside a single coarse cell has $n_x - 1$ subgrid acceleration nodes and n_x pressure nodes, each block T is of size $(n_x - 1) \times n_x$. Finally B^f can be written as the block diagonal matrix with blocks given by T. ∎

LEMMA 6. *The matrix B^c is an upper bidiagonal $(K - 1) \times K$ block matrix. The blocks are of size $1 \times N$ and are given by*

$$B^c_{l,l} = \frac{h_x h_y}{H_x} \begin{bmatrix} 1 & \dots & 1 \end{bmatrix}, \qquad B^c_{l,l+1} = -\frac{h_x h_y}{H_x} \begin{bmatrix} 1 & \dots & 1 \end{bmatrix}. \tag{2.44}$$

Proof. The entries of the matrix B^c are the inner products of the x derivative of coarse acceleration basis functions and pressure basis functions (2.14). The total number of the coarse acceleration nodes is $(K-1)$ and the total number of the pressure nodes is NK, so B^c has size $(K-1)\times NK$. Each coarse acceleration basis function is supported on two coarse cells and, therefore, has a nonzero inner product only with the pressure basis functions internal to those cells. If we introduce the blocks B^c_{ij} of size $1\times N$ which represent the interaction of the ith coarse basis function with the pressure basis functions from the jth coarse cell, then the matrix B^c can be written as a bidiagonal matrix:

$$B^c = \begin{bmatrix} B^c_{1,1} & B^c_{1,2} & & & 0 \\ & B^c_{2,2} & B^c_{2,3} & & \\ & & \ddots & \ddots & \\ 0 & & & B^c_{K-1,K-1} & B^c_{K-1,K} \end{bmatrix}. \tag{2.45}$$

The entries of B^c can be computed exactly. To evaluate $(b^c)_{l,m} = \langle w_m, \frac{\partial (u^c_x)_l}{\partial x}\rangle$, we use the fact that $(u^c_x)_l$ is a linear function in x and a constant in y. Thus, its derivative is easily computed and is given by

$$\frac{\partial (u^c_x)_l}{\partial x} = \begin{cases} \dfrac{1}{H_x} & l\text{th coarse cell,} \\ -\dfrac{1}{H_x} & (l+1)\text{th coarse cell.} \end{cases} \tag{2.46}$$

The pressure basis function w_m is 1 on the corresponding fine cell and 0 everywhere else. Therefore, we have

$$b^c_{l,m} = \left\langle w_m, \frac{\partial (u^c_x)_l}{\partial x} \right\rangle = \begin{cases} (h_x h_y)\dfrac{1}{H_x} & l\text{th coarse cell,} \\ -(h_x h_x)\dfrac{1}{H_x} & (l+1)\text{th coarse cell.} \end{cases} \tag{2.47}$$

Thus,

$$B^c_{l,l} = \frac{h_x h_y}{H_x}\begin{bmatrix} 1 & \dots & 1 \end{bmatrix}, \qquad B^c_{l,l+1} = -\frac{h_x h_y}{H_x}\begin{bmatrix} 1 & \dots & 1 \end{bmatrix}. \tag{2.48}$$ ∎

Proof of formula (2.23)–(2.24) *for* D. We can use Lemmas 2, 3, 5, and 6 to study the matrix D, which is given by formula (2.41). Performing block multiplication in $(A^{cf})^T(A^{ff})^{-1}B^f$, we see that the resulting matrix is an upper bidiagonal block matrix. Let us derive explicit formulas for the diagonal blocks first. The results obtained in Lemmas 2, 3, and 5 give that

$$\begin{aligned} &[(A^{cf})^T(A^{ff})^{-1}B^f]_{ii} \\ &\quad = \begin{bmatrix} (u^c_x)_i\big|_{(M(i-1)+1}, & (u^c_x)_i\big|_{M(i-1)+2}, & \dots & (u^c_x)_i\big|_{Mi} \end{bmatrix} \begin{bmatrix} T & & & 0 \\ & T & & \\ & & \ddots & \\ 0 & & & T \end{bmatrix}, \end{aligned} \tag{2.49}$$

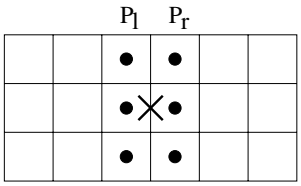

FIG. 2.6. *The nodes of coarse acceleration and pressure involved in the difference equation.*

where $(u_x^c)_i\big|_l$, $l = M(i-1)+1, M(i-1)+2, \ldots, Mi$, are the values of the coarse basis function at the nodal points of subgrid acceleration inside coarse cell i. Note that these values can be easily computed since the function $(u_x^c)_i$ is known (it is linear in x and constant in y, and it takes value 1 at the corresponding node and 0 at all other nodes).

After further matrix multiplications and application of Lemma 6, we see that D is block upper bidiagonal with the blocks given by (2.23)–(2.24). The nonzero entries correspond to those pressure nodes that are located along the boundary of the coarse cell i. □

2.3. Difference and differential equations for coarse acceleration. The results of Theorem 1 allow us to write the difference equation for the coarse acceleration explicitly as

$$(h_x h_y)\sum_{l=1}^{n_y}\rho_l^i(\mathbf{v_x^c})_i = -(h_x h_y)\left[\sum_{l=1}^{n_y}\frac{\mathbf{p}_{Ni+n_x(l-1)+1}}{h_x} - \sum_{l=1}^{n_y}\frac{\mathbf{p}_{N(i-1)+n_x l}}{h_x}\right]. \tag{2.50}$$

Notice that the two sums on the right-hand side of (2.50) are the sums of the pressure values to the right and to the left of the coarse cell boundary on which coarse acceleration $(\mathbf{v_x^c})_i$ is located (Figure 2.6). If we denote the average of pressure along the right and left boundary, respectively, by

$$\bar{\mathbf{p}}_r \equiv \frac{\sum_{l=1}^{n_y}\mathbf{p}_{Ni+n_x(l-1)+1}}{n_y}, \qquad \bar{\mathbf{p}}_l \equiv \frac{\sum_{l=1}^{n_y}\mathbf{p}_{N(i-1)+n_x l}}{n_y}, \tag{2.51}$$

then (2.50) reduces to

$$\bar{\rho}(\mathbf{v_x^c})_i = -\frac{\bar{\mathbf{p}}_r - \bar{\mathbf{p}}_l}{h_x}, \tag{2.52}$$

where $\bar{\rho}$ is the average of the density values on the boundary of the coarse cell, i.e.,

$$\bar{\rho} = \frac{\sum_{l=1}^{n_y}\rho_l^i}{n_y}.$$

Let us define a new function ρ^{ups}, which we will call upscaled density. This function is defined to be the original density values at node points interior to the coarse cells and is an average of density values $\bar{\rho}$ at node points along coarse block edges. In the following theorem, we derive the continuous differential equation for v_x^c and p.

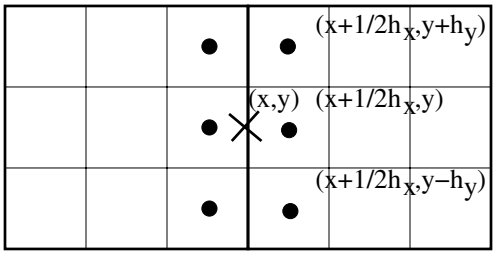

FIG. 2.7. *The coordinates of coarse acceleration and pressure involved in the difference equation in the case of* 3×3 *fine cells inside a single coarse cell.*

THEOREM 7. *Assume pressure* p *is at least four times continuously differentiable. Then the difference equation* (2.52) *is a discretization of the following differential equation*

$$\rho^{ups} v_x^c = -\frac{\partial p}{\partial x},$$

with order of approximation $O(h_x^2 + h_y^2)$.

Note. Theorem 7 gives a continuous differential equation for coarse acceleration which is essentially (2.1) from the original first-order system with density replaced by an upscaled density. We see that the upscaled acceleration approximates the gradient of pressure on the boundaries of coarse cells and, thus, compensates for the simplifying zero boundary conditions used in the algorithm.

Proof. Let acceleration node $(\mathbf{v_x^c})_\mathbf{i}$ be associated with the point (x, y). Replace $(\mathbf{v_x^c})_\mathbf{i}$, $\mathbf{p}_{Ni+n_x(l-1)+1}$, and $\mathbf{p}_{N(i-1)+n_x l}$ in the difference equation by the smooth functions v_x^c and p at the corresponding points and expand each pressure term in a Taylor series about the point (x, y). Notice that the pressure terms in $\bar{\mathbf{p}}_r$ are located at $(x + \frac{1}{2}h_x, y \pm jh_y)$, where jh_y is the distance between the corresponding pressure node and the acceleration node in the y direction. For example, in the case of 3×3 fine cells inside a single coarse cell, we see in Figure 2.7 that the terms in the sum $\bar{\mathbf{p}}_r$ are located at $(x + \frac{1}{2}h_x, y + h_y)$, $(x + \frac{1}{2}h_x, y)$, and $(x + \frac{1}{2}h_x, y - h_y)$. Thus, the subscript j takes on values $j = 0, 1$. Similarly, the pressure terms in $\bar{\mathbf{p}}_l$ are located at $(x - \frac{1}{2}h_x, y \pm jh_y)$. We expand each pressure term in (2.51) in a fourth-order Taylor series about (x, y). Since the pressure nodes are symmetric about the point (x, y), the linear and cubic terms in h_y cancel when computing the sums in (2.51), and we obtain for $\bar{\mathbf{p}}_r$ and $\bar{\mathbf{p}}_l$

(2.53)
$$\bar{\mathbf{p}}_r = \frac{\displaystyle\sum_{l=1}^{n_y} \left[p + \frac{\partial p}{\partial x}\left(\frac{1}{2}h_x\right) + \frac{1}{2}\left[\frac{\partial^2 p}{\partial x^2}\left(\frac{1}{2}h_x\right)^2 + \frac{\partial^2 p}{\partial y^2}(jh_y)^2\right]\right]}{n_y} + O(h_x^3) + O(h_x h_y^2)$$

and

(2.54)
$$\bar{\mathbf{p}}_l = \frac{\displaystyle\sum_{l=1}^{n_y} \left[p - \frac{\partial p}{\partial x}\left(\frac{1}{2}h_x\right) + \frac{1}{2}\left[\frac{\partial^2 p}{\partial x^2}\left(\frac{1}{2}h_x\right)^2 + \frac{\partial^2 p}{\partial y^2}(jh_y)^2\right]\right]}{n_y} + O(h_x^3) + O(h_x h_y^2),$$

where $p \equiv p(x, y)$. Substituting (2.53) and (2.54) into the difference equation (2.52) results in the following differential equation:

$$\rho^{ups} v_x^c = -\frac{\partial p}{\partial x}, \tag{2.55}$$

up to order $O(h_x^2 + h_y^2)$. We conclude that the upscaled acceleration approximates the x derivative of pressure on the boundary of the coarse cell with the upscaled density given by $\bar{\rho}$ at each nodal point. ∎

2.4. Matrix analysis of the pressure equation. In the next two sections, we will explain how coarse acceleration determines pressure in the time-dependent equation ((2.6) of the subgrid problem). The upscaling algorithm modifies the original wave equation on the boundaries of the coarse cells by using the coarse acceleration and the averaged density values on these boundaries. The equation which is solved includes an additional cross-derivative term not seen in the original wave equation. We follow the same basic outline as in sections 2.2–2.3. In other words, we start by analyzing the matrix form of (2.6) and then make use of results from the previous sections to derive the matrix equation for coarse acceleration and pressure. These results are then used to obtain a corresponding difference and finally differential equation for pressure resulting from the upscaling algorithm.

THEOREM 8. *Consider the set of subgrid problems* (2.5)–(2.6). *The elimination of the subgrid unknowns from the pressure equation* (2.6) *results in the following linear system for the coarse acceleration and pressure*

$$W \frac{\partial^2 \mathbf{p}}{\partial t^2} = -D^T \mathbf{v_x^c} - C\mathbf{p} - (v_y \text{ terms}) + F.$$

The matrix D and vector F are defined in Theorem 1 *by* (2.23), (2.24), *and* (2.14). *The matrix W is diagonal with entries having values of $\frac{1}{\rho c^2}$ at the corresponding pressure nodes. The matrix C is a block diagonal matrix. The blocks of C are of size $n_x \times n_x$ and are given by*

$$C_{i,i} = \frac{h_x h_y}{h_x^2} \begin{bmatrix} \rho_{I+1}^{-1} & -\rho_{I+1}^{-1} & & & 0 \\ -\rho_{I+1}^{-1} & \rho_{I+1}^{-1} + \rho_{I+2}^{-1} & -\rho_{I+2}^{-1} & & \\ \ddots & \ddots & \ddots & & \\ & & & & \\ & -\rho_{I+n_x-2}^{-1} & \rho_{I+n_x-2}^{-1} + \rho_{I+n_x-1}^{-1} & -\rho_{I+n_x-1}^{-1} & \\ 0 & & -\rho_{I+n_x-1}^{-1} & \rho_{I+n_x-1}^{-1} & \end{bmatrix}, \tag{2.56}$$

where $I = (i-1)(n_x - 1)$.

Proof. The idea of the proof is similar to that of Theorem 1. First, we use the matrix form of the subgrid problem (2.15)–(2.16) to eliminate the subgrid unknowns from the pressure equation (2.16). We obtain the time-dependent matrix equation for pressure and coarse acceleration only and derive explicit formulas for the matrix entries.

Recall that the matrix form of the subgrid problem is given by (2.15)–(2.16). We see that the first equation can be solved easily for $\delta \mathbf{v_x}$ in terms of $\mathbf{v_x^c}$. Thus, we can eliminate the subgrid unknowns from the time-dependent pressure equation. We

obtain

(2.57)
$$W\frac{\partial^2 \mathbf{p}}{\partial t^2} = -[(B^c)^T - (B^f)^T(A^{ff})^{-1}A^{cf}]\mathbf{v}_\mathbf{x}^\mathbf{c} - (B^f)^T(A^{ff})^{-1}B^f\mathbf{p} - (v_y \text{ terms}) + F,$$

or

$$W\frac{\partial^2 \mathbf{p}}{\partial t^2} = -D^T\mathbf{v}_\mathbf{x}^\mathbf{c} - C\mathbf{p} - (v_y \text{ terms}) + F. \tag{2.58}$$

In the rest of the proof of the theorem, we discuss the structure and entries of the matrices W, D^T, and C. In what follows, if i is the ith pressure node, then $\frac{1}{\rho c^2}\big|_i$ denotes the value of $\frac{1}{\rho c^2}$ at that node.

LEMMA 9. *The matrix W is a diagonal $NK \times NK$ matrix with nonzero entries given by*

$$w_{i,i} = (h_x h_y)\frac{1}{\rho c^2}\Big|_i. \tag{2.59}$$

Proof. The entries of the matrix W are the inner products of pressure basis functions with themselves, $\langle \frac{1}{\rho c^2} w_i, w_j \rangle$. Computing these entries using the midpoint rule and noting that each pressure basis function is supported on one fine cell only gives the desired result. ∎

Completion of the proof of Theorem 8. Let us now consider the matrix for coarse acceleration D^T. Notice that the matrix D was defined in Theorem 1 (2.23)–(2.24). Using those results, we see that D^T is a lower block bidiagonal matrix with blocks given by $D^T_{i,i+1}$ and $D^T_{i,i}$. The nonzero entries in D^T are associated with pressure unknowns located along the vertical boundaries of the coarse cells.

Let us now turn our attention to the coefficient matrix for pressure

$$C = (B^f)^T(A^{ff})^{-1}B^f.$$

The structure and the entries of A^{ff} and B^f were discussed in Lemmas 3 and 5. We have shown that A^{ff} is a diagonal matrix, and B^f is a block diagonal matrix with blocks of size $(n_x - 1) \times n_x$. Thus, C is also a block diagonal matrix with blocks of size $n_x \times n_x$.

We can derive explicit formulas for the entries of C. For simplicity of notation, let us discuss the derivation of the first block $C_{1,1}$. Using the explicit formulas for the entries of A^{ff} and the blocks of B^f in (2.29) and (2.42), we obtain

(2.60) $C_{1,1}$

$$= \frac{h_x h_y}{h_x^2}\begin{bmatrix} -1 & 0 & \dots & 0 \\ 1 & -1 & \dots & 0 \\ 0 & 1 & \dots & 0 \\ & \dots & \dots & \\ 0 & 0 & \dots & 1 \end{bmatrix}\begin{bmatrix} \rho_1^{-1} & & & 0 \\ & \ddots & & \\ 0 & & & \rho_{n_x-1}^{-1} \end{bmatrix}\begin{bmatrix} -1 & 1 & 0 & \dots & 0 & 0 \\ 0 & -1 & 1 & \dots & 0 & 0 \\ & & \dots & \dots & & \\ 0 & 0 & 0 & \dots & -1 & 1 \end{bmatrix}$$

$$= \frac{h_x h_y}{h_x^2}\begin{bmatrix} \rho_1^{-1} & -\rho_1^{-1} & 0 & \dots & 0 & 0 & 0 \\ -\rho_1^{-1} & \rho_1^{-1} + \rho_2^{-1} & -\rho_2^{-1} & \dots & 0 & 0 & 0 \\ & & & \dots & & & \\ 0 & 0 & 0 & \dots & -\rho_{n_x-2}^{-1} & \rho_{n_x-2}^{-1} + \rho_{n_x-1}^{-1} & -\rho_{n_x-1}^{-1} \\ 0 & 0 & 0 & \dots & 0 & -\rho_{n_x-1}^{-1} & \rho_{n_x-1}^{-1} \end{bmatrix}.$$

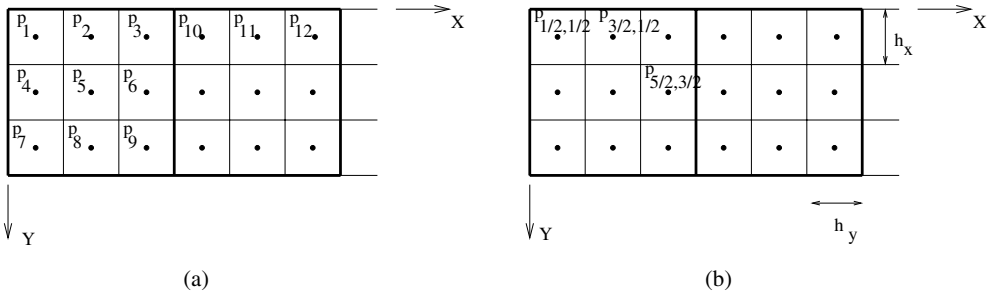

FIG. 2.8. *Pressure unknowns in the case of* 3×3 *fine cells inside a single coarse cell:* (a) *vector notation,* (b) *coordinate notation.*

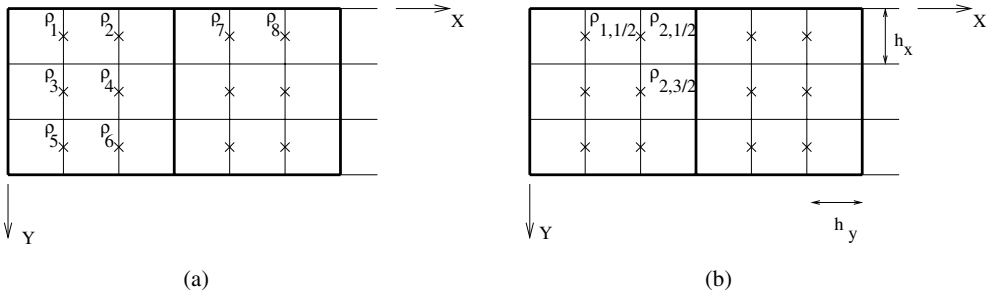

FIG. 2.9. *Density values at subgrid velocity nodes in the case of* 3×3 *fine cells inside a single coarse cell:* (a) *vector notation,* (b) *coordinate notation.*

Similarly, we can compute the rest of the blocks $C_{i,i}$ to get (2.56). Recall that blocks of C have size $n_x \times n_x$, so each block is associated with one row of pressure unknowns inside a single coarse cell. □

2.5. Difference and differential equations for pressure. To better understand the meaning of the matrix problem (2.58), we interpret it as a difference equation first and then as a continuous differential equation. In the following theorems, it is beneficial to change from vector notation (Figures 2.8(a) and 2.9(a)), used in the previous sections, to a spatial coordinate notation (Figures 2.8(b) and 2.9(b)). This notation change simplifies the discussion of the difference equation. In coordinate notation, $p_{i+1/2,j+1/2}$ will denote the value of pressure at the grid point $(x_{i+1/2} = (i + 1/2)h_x$, $y_{j+1/2} = (j + 1/2)h_y)$, and $\rho_{i,j+1/2}$ will be the value of density at the grid point $(x_i = ih_x,\ y_{j+1/2} = (j + 1/2)h_y)$, which is associated with the subgrid acceleration node (Figure 2.9). In the following theorems, we see that the matrix problem gives rise to different difference equations and hence different differential equations at different points in the spatial grid. The three pressure node locations we need to consider are (a) nodes internal to the coarse cell, (b) nodes along the right boundary of the coarse cell, and (c) nodes along the left boundary of the coarse cell (Figure 2.10).

In Theorem 10, we derive the difference and differential equations for the internal pressure nodes (Figure 2.10(a)). We then derive the difference and differential equations for the pressure nodes along the right boundary in Theorem 11. The result for pressure nodes along the left boundary of the coarse cells is similar.

THEOREM 10. *Let* $p_{i+1/2,j+1/2}$ *be a pressure unknown internal to a particular coarse cell (Figure* 2.10(a)*). Then the difference equation corresponding to matrix*

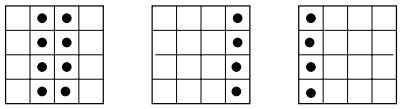

FIG. 2.10. *Three pressure node locations inside one coarse cell:* (a) *internal pressure nodes,* (b) *pressure nodes along the right boundary of the coarse cell,* (c) *pressure nodes along the left boundary of the coarse cell.*

problem (2.58) *has the following form:*

$$\begin{aligned}(2.61)\quad &\frac{1}{\rho c^2}\frac{\partial^2 p_{i+1/2,j+1/2}}{\partial t^2}\\ &= -\frac{1}{h_x^2}\Big(- p_{i+3/2,j+1/2}\rho^{-1}_{i+1,j+1/2} + p_{i+1/2,j+1/2}\left(\rho^{-1}_{i+1,j+1/2} + \rho^{-1}_{i,j+1/2}\right)\\ &\qquad\qquad - p_{i-1/2,j+1/2}\rho^{-1}_{i,j+1/2}\Big)\\ &\quad - \frac{1}{h_y^2}\Big(- p_{i+1/2,j+3/2}\rho^{-1}_{i+1/2,j+1} + p_{i+1/2,j+1/2}\left(\rho^{-1}_{i+1/2,j+1} + \rho^{-1}_{i+1/2,j}\right)\\ &\qquad\qquad - p_{i+1/2,j-1/2}\rho^{-1}_{i+1/2,j}\Big) + f_{i+1/2,j+1/2}.\end{aligned}$$

Further, assume pressure p *and density* ρ *are at least four times continuously differentiable. Then difference equation* (2.61) *is a discretization of the following continuous differential equation:*

$$(2.62)\qquad \frac{1}{\rho c^2}\frac{\partial^2 p}{\partial t^2} = \frac{\partial}{\partial x}\left(\rho^{-1}\frac{\partial p}{\partial x}\right) + \frac{\partial}{\partial y}\left(\rho^{-1}\frac{\partial p}{\partial y}\right) + f,$$

with order of approximation $O(h_x^2 + h_y^2)$.

Proof. Recall that the matrix equation for the pressure and coarse acceleration is given by (2.58). For simplicity, let us consider a particular case of 3×3 fine cells inside a single coarse cell (that is, $n_x = n_y = 3$), and we will focus initially on a particular pressure unknown, $p_{3/2,1/2}$, internal to the first coarse cell (Figure 2.8). Notice that in this case each coarse cell contains only three internal pressure unknowns. We chose $p_{3/2,1/2}$, since it is the only internal unknown in the first row of the first coarse cell. We first derive a difference equation for this unknown and then generalize the resulting formula. Since W is diagonal and its entries are given by (2.59) (Lemma 9), the product $W\frac{\partial^2 \mathbf{p}}{\partial t^2}$ yields

$$(2.63)\qquad (h_x h_y)\frac{1}{\rho c^2}\Big|_{3/2,1/2}\frac{\partial^2 p_{3/2,1/2}}{\partial t^2}.$$

As was shown in Theorem 8, the corresponding row of the matrix D^T contains zeroes. Therefore, the difference equation does not involve the coarse acceleration nodes. Let us now consider the term $C\mathbf{p}$. Since the unknown of interest is located in the first row of the first coarse cell, we need to consider the block $C_{1,1}$ (2.60). In the case where

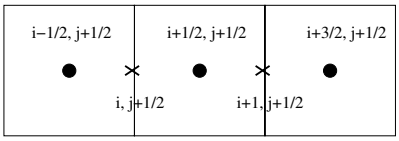

FIG. 2.11. *Finite-difference stencil for the internal pressure unknowns. Note that pressure nodes are denoted by circles and acceleration nodes by x's. Density lives at acceleration nodes, sound velocity at pressure nodes.*

$n_x = n_y = 3$, $C_{1,1}$ becomes

$$C_{1,1} = \frac{h_x h_y}{h_x^2} \begin{bmatrix} \rho_{1,1/2}^{-1} & -\rho_{1,1/2}^{-1} & 0 \\ -\rho_{1,1/2}^{-1} & \rho_{1,1/2}^{-1} + \rho_{2,1/2}^{-1} & -\rho_{2,1/2}^{-1} \\ 0 & -\rho_{2,1/2}^{-1} & \rho_{2,1/2}^{-1} \end{bmatrix}, \tag{2.64}$$

where we have used coordinate notation (Figure 2.9). The pressure unknown $p_{3/2,1/2}$ corresponds to the second entry in the vector $\mathbf{p}$. Thus, multiplying the second row of the matrix C by $\mathbf{p}$, we obtain a sum of three nonzero terms

$$\frac{h_x h_y}{h_x^2} \left(-p_{1/2,1/2} \rho_{1,1/2}^{-1} + p_{3/2,1/2} \left(\rho_{2,1/2}^{-1} + \rho_{1,1/2}^{-1} \right) - p_{5/2,1/2} \rho_{2,1/2}^{-1} \right). \tag{2.65}$$

Putting (2.63) and (2.65) together gives

$$\begin{aligned} \frac{1}{\rho c^2}\Big|_{3/2,1/2} \frac{\partial^2 p_{3/2,1/2}}{\partial t^2} = \frac{1}{h_x^2} \Big(& -p_{1/2,1/2} \rho_{1,1/2}^{-1} + p_{3/2,1/2} \left(\rho_{2,1/2}^{-1} + \rho_{1,1/2}^{-1} \right) - p_{5/2,1/2} \rho_{2,1/2}^{-1} \Big) \\ & - (v_y \text{ terms}) + f_{3/2,1/2}. \end{aligned} \tag{2.66}$$

The above formula can be generalized to the case of $n_x \times n_y$ fine cells inside a coarse cell. Since the structure of the matrices does not change, the same steps will lead us to the following difference equation for internal pressure unknowns (see Figure 2.11 for the x-derivative finite difference stencil):

$$\begin{aligned} & \frac{1}{\rho c^2} \frac{\partial^2 p_{i+1/2,j+1/2}}{\partial t^2} \\ & = -\frac{1}{h_x^2} \Big(- p_{i+3/2,j+1/2} \rho_{i+1,j+1/2}^{-1} + p_{i+1/2,j+1/2} \left(\rho_{i+1,j+1/2}^{-1} + \rho_{i,j+1/2}^{-1} \right) \\ & \qquad - p_{i-1/2,j+1/2} \rho_{i,j+1/2}^{-1} \Big) - (v_y \text{ terms}) + f_{i+1/2,j+1/2}. \end{aligned} \tag{2.67}$$

The difference expression for the v_y terms is similar.

Notice that the first term on the right-hand side of (2.67) is the standard second-order centered finite difference approximation of $\frac{\partial}{\partial x}(\rho^{-1} \frac{\partial p}{\partial x})$ [11]. Expanding the pressure and density terms in Taylor series around the point $(x_{i+1/2}, y_{j+1/2})$, we obtain from (2.67)

$$\frac{1}{\rho c^2} \frac{\partial^2 p}{\partial t^2} = \frac{\partial}{\partial x} \left(\rho^{-1} \frac{\partial p}{\partial x} \right) + \frac{\partial}{\partial y} \left(\rho^{-1} \frac{\partial p}{\partial y} \right) + f + O(h_x^2 + h_y^2). \tag{2.68}$$

This shows that the difference equation for the pressure unknowns internal to the coarse cell, which results from the upscaling algorithm, approximates the standard continuous acoustic wave equation up to order $O(h_x^2 + h_y^2)$. □

THEOREM 11. *Let $p_{i+1/2,j+1/2}$ be a pressure unknown located along the right boundary of a particular coarse cell (Figure* 2.10(b)*). Then the difference equation corresponding to* (2.58) *has the following form:*

(2.69)
$$\begin{aligned}
&\frac{1}{\rho c^2}\frac{\partial^2 p_{i+1/2,j+1/2}}{\partial t^2} \\
&= -\frac{1}{h_x}v_x^c - \frac{1}{h_x^2}\left(p_{i+1/2,j+1/2}\rho^{-1}_{i,j+1/2} - p_{i-1/2,j+1/2}\rho^{-1}_{i,j+1/2}\right) \\
&\quad -\frac{1}{h_y^2}\Big(- p_{i+1/2,j+3/2}\rho^{-1}_{i+1/2,j+1} + p_{i+1/2,j+1/2}\left(\rho^{-1}_{i+1/2,j+1} + \rho^{-1}_{i+1/2,j}\right) \\
&\qquad\qquad -p_{i+1/2,j-1/2}\rho^{-1}_{i+1/2,j}\Big) + f_{i+1/2,j+1/2},
\end{aligned}$$

where v_x^c is the value of the coarse acceleration on the given boundary.

Further, assume pressure p and density ρ are at least four times continuously differentiable. Then difference equation (2.69) *is a discretization of the following continuous differential equation with order of approximation $O(h_x + h_y)$:*

(2.70)
$$\frac{1}{\rho c^2}\frac{\partial^2 p}{\partial t^2} = \frac{\partial}{\partial x}\left((\rho^{ups})^{-1}\frac{\partial p}{\partial x}\right) + \left((\rho^{ups})^{-1}\frac{\partial^2 p}{\partial x \partial y}\right)K + \frac{\partial}{\partial y}\left((\rho^{ups})^{-1}\frac{\partial p}{\partial y}\right) + f,$$

where K is a constant which depends on the location of the pressure node within a single coarse cell.

Proof. The proof of the theorem is similar to that of Theorem 10. We first consider the case of 3×3 fine cells inside a single coarse cell and derive the difference equation for pressure unknown, $p_{5/2,1/2}$ located along the right boundary of the coarse cell (Figure 2.8(b)). The pressure unknown $p_{5/2,1/2}$ corresponds to the third entry in the vector $\mathbf{p}$ (Figure 2.8). Therefore, we need to look at the third rows of the matrices D^T and C. Only the first entry of the third row of D^T is nonzero (Theorems 1 and 8). The third row of the block $C_{1,1}$ in coordinate notation is given by (2.64). Thus, performing matrix-vector multiplications in matrix problem (2.58), we obtain

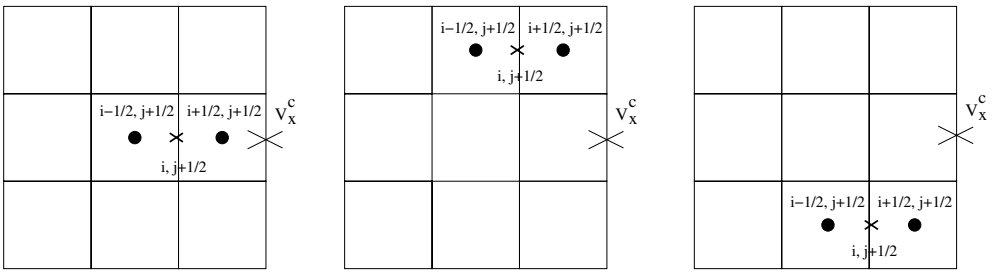

FIG. 2.12. *Locations of pressure nodes relative to coarse velocity for the case of 3×3 fine cells inside a single coarse cell. Note that pressure nodes are denoted by circles and subgrid and coarse acceleration nodes by x's and X's, respectively. Density lives at the same location as the subgrid acceleration nodes.*

the difference equation for $p_{5/2,1/2}$:

$$\frac{1}{\rho c^2}\frac{\partial^2 p_{5/2,1/2}}{\partial t^2} = -\frac{1}{h_x}v_x^c - \frac{1}{h_x^2}\left(p_{5/2,1/2}\rho_{2,1/2}^{-1} - p_{3/2,1/2}\rho_{2,1/2}^{-1}\right) - (v_y \text{ terms}) + f_{5/2,1/2}. \tag{2.71}$$

The above formula can be generalized to the case of $n_x \times n_y$ fine cells inside a coarse cell. We obtain the following difference equation for pressure unknowns along the boundary of the coarse cell (see Figure 2.12)

$$\frac{1}{\rho c^2}\frac{\partial^2 p_{i+1/2,j+1/2}}{\partial t^2} = -\frac{1}{h_x}v_x^c - \frac{1}{h_x^2}\left(p_{i+1/2,j+1/2}\rho_{i,j+1/2}^{-1} - p_{i-1/2,j+1/2}\rho_{i,j+1/2}^{-1}\right) - (v_y \text{ terms}) + f_{i+1/2,j+1/2}, \tag{2.72}$$

where v_x^c is the coarse acceleration unknown on the given boundary.

Let us now derive the differential equation. The idea is to use Taylor expansions around the point $(x_{i+1/2}, y_{j+1/2})$. First, consider the term v_x^c on the right-hand side of (2.72). We have shown in the previous sections that coarse acceleration is related to pressure through the difference equation

$$v_x^c = -\frac{1}{\bar\rho}\frac{\bar p_r - \bar p_l}{h_x}. \tag{2.73}$$

The terms $\bar p_r$, $\bar p_l$ are the averaged sums of pressure unknowns to the right and left of a particular boundary of the coarse cell, and $\bar\rho$ is the average of density values on the same boundary. We can write $\bar p_r$, $\bar p_l$, and $\bar\rho$ using coordinate notation as

$$\bar p_r = \frac{\sum_k p_{i+3/2,j+1/2+k}}{n_y}, \qquad \bar p_l = \frac{\sum_k p_{i+1/2,j+1/2+k}}{n_y}, \tag{2.74}$$

$$\bar\rho = \frac{\sum_k \rho_{i+1,j+1/2+k}}{n_y}, \tag{2.75}$$

where $p_{i+3/2,j+1/2+k} = p(h_x(i+3/2), h_y(j+1/2+k))$, $\rho_{i+1,j+1/2+k} = \rho(h_x(i+1), h_y(j+1/2+k))$, and kh_y represents the distance between the unknown and the point $(x_{i+1/2}, y_{j+1/2})$ in the y direction. The number of terms in each sum is equal to n_y, the number of fine cells inside a single coarse cell in the y direction. The values that k takes will depend on the number of fine cells inside a single coarse cell and the location of a particular pressure unknown in that cell. For example, Figure 2.13 shows that in the 3×3 case, if the pressure unknowns of interest are in bold, then k may take values -1, 0, 1 (Figure 2.13(a)); or the values 0, 1, 2 (Figure 2.13(b)); or 0, -1, -2 (Figure 2.13(c)). Expanding all the pressure unknowns in $\bar p_r$, $\bar p_l$ in a fourth-order Taylor series about the point $(x_{i+1/2}, y_{j+1/2})$ and using (2.73), we obtain for coarse acceleration

$$v_x^c = -\frac{1}{\bar\rho}\left[\frac{\partial p}{\partial x} + \frac{h_x}{2}\frac{\partial^2 p}{\partial x^2} + \frac{\sum_k k}{n_y}h_y\frac{\partial^2 p}{\partial x \partial y}\right] + O(h_x^2 + h_x h_y + h_y^2), \tag{2.76}$$

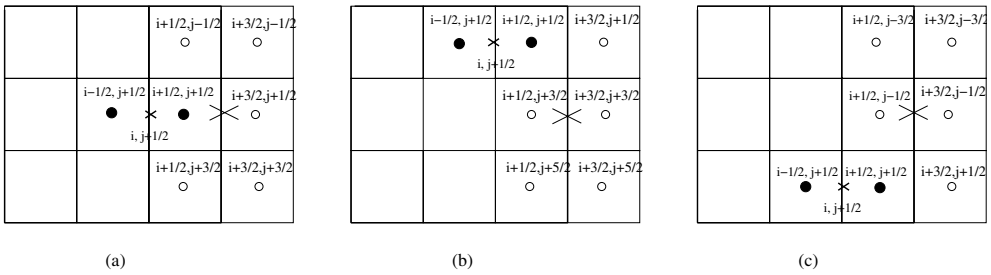

FIG. 2.13. *Examples of finite-difference stencils for different positions of pressure unknown* $p_{i+1/2,j+1/2}$ *in the case of* 3×3 *fine cells inside a single coarse cell. The open circles denote the pressure unknowns used in the calculation of* $\bar{p}_r$ *and* $\bar{p}_l$.

where $p \equiv p(x_{i+1/2}, y_{j+1/2})$. Expanding the rest of the terms on the right-hand side of (2.72) around the same point, we obtain

$$
\begin{aligned}
(2.77)\quad & -\frac{1}{h_x} v_x^c - \frac{1}{h_x^2}\left(p_{i+1/2,j+1/2}\rho^{-1}_{i,j+1/2} - p_{i-1/2,j+1/2}\rho^{-1}_{i,j+1/2}\right) \\
&\qquad = \frac{1}{\bar{\rho}}\left(\frac{1}{h_x}\frac{\partial p}{\partial x} + \frac{1}{2}\frac{\partial^2 p}{\partial x^2} + \frac{\sum\limits_k k}{n_y}\frac{h_y}{h_x}\frac{\partial^2 p}{\partial x \partial y}\right) \\
&\qquad\quad - \left(\frac{1}{h_x}\frac{\partial p}{\partial x} - \frac{1}{2}\frac{\partial^2 p}{\partial x^2}\right) \times \left(\rho^{-1} - \frac{h_x}{2}\frac{\partial \rho^{-1}}{\partial x}\right) + O(h_x + h_y),
\end{aligned}
$$

where $\rho \equiv \rho(x_{i+1/2}, y_{j+1/2})$. We can use the definition of the new function ρ^{ups} to say that

$$
(2.78)\qquad \frac{1}{\bar{\rho}} = \left(\rho^{ups}_{i+1,j+1/2}\right)^{-1}.
$$

Suppose the function ρ^{ups} can be constructed in such a way that it is smooth enough for Taylor series expansion. Expanding $(\rho^{ups}_{i+1,j+1/2})^{-1}$ around the point $(x_{i+1/2}, y_{j+1/2})$, we obtain from (2.77)

$$
\begin{aligned}
(2.79)\quad & -\frac{1}{h_x} v_x^c - \frac{1}{h_x^2}\left(p_{i+1/2,j+1/2}\rho^{-1}_{i,j+1/2} - p_{i-1/2,j+1/2}\rho^{-1}_{i,j+1/2}\right) \\
&\qquad = \frac{\partial p}{\partial x}\frac{\partial (\rho^{ups})^{-1}}{\partial x} + \frac{\partial^2 p}{\partial x^2}(\rho^{ups})^{-1} + \frac{\sum\limits_k k}{n_y}\frac{h_y}{h_x}\frac{\partial^2 p}{\partial x \partial y}(\rho^{ups})^{-1} + O(h_x + h_y).
\end{aligned}
$$

We use (2.79) in (2.72) to obtain the following differential equation

$$
(2.80)\qquad \frac{1}{\rho c^2}\frac{\partial^2 p}{\partial t^2} \;=\; \frac{\partial}{\partial x}\left((\rho^{ups})^{-1}\frac{\partial p}{\partial x}\right) + \left((\rho^{ups})^{-1}\frac{\partial^2 p}{\partial x \partial y}\right) K + (v_y \text{ terms}) + f,
$$

$$
\text{where } K = \frac{\sum\limits_k k}{n_y}\frac{h_y}{h_x}.
$$

Note. The constant K depends on the size of the fine mesh, the size of the coarse mesh, and the position of the pressure node under consideration. In particular, $K = 0$ when the pressure node has the same y coordinate as the coarse acceleration node. In this situation, k takes values $-1, 0, 1$, so that $\sum_k k = 0$ (see Figure 2.13(a)). ∎

3. Conclusions. To model subsurface phenomena ranging from the centimeter to the kilometer scale (micro- to macroscale), requires enormous amounts of computing power. Resolving all fine-scale features over large sections of the earth (at depths ranging from the near-surface down to the deep crust) is computationally prohibitive. Upscaling techniques allow us to perform these simulations on a coarser scale while capturing some of this fine-scale subwavelength information. There are a variety of upscaling methods. However, most of these techniques have been developed in the context of elliptic equations. We have adapted the operator-based upscaling technique, previously developed for elliptic flow, to the variable density, variable sound velocity acoustic wave equation. The upscaling method relies on decomposing the space of unknowns into coarse and subgrid subspaces. The problem is then naturally solved in two steps. First, we solve the subgrid problems for fine-scale information internal to each coarse cell. Then we use the subgrid solutions to augment the coarse-scale operator. A simplifying zero boundary condition imposed on each coarse cell decouples the subgrid problems from one coarse cell to the next. The fine-grid input parameters (density and sound velocity) are used throughout the computations. The algorithm does not explicitly average these input parameters. Further, separation of scales is not assumed with this technique. The numerical implementation of the upscaling algorithm for the wave equation is discussed in detail in Vdovina et al. [17]. Numerical experiments presented in that paper indicate that operator-based upscaling models wave propagation (even at the subwavelength scale) quite accurately relative to full finite difference solutions.

In this paper we convert the second-order acoustic wave equation into a system of two first-order equations (first-order in space) which involve solving for both pressure and its gradient (acceleration). The algorithm is based conceptually on the mixed finite element method. However, the pressure equation is solved via finite differences due to an equivalence between finite elements and finite differences. The first practical result from this analysis is that the system matrix for coarse acceleration is diagonal which greatly simplifies the implementation of the method.

Even more importantly, the analysis presented in this paper gives the first explanation of exactly which physical equations are solved by the upscaling algorithm. What we have shown is that the upscaling algorithm produces a coarse solution to the original constitutive equation for acceleration with the input density field redefined as an averaged density along coarse-block edges. This result indicates that the algorithm compensates for the simplifying zero boundary conditions on coarse block edges. Similarly, the upscaling algorithm leaves the wave equation for pressure untouched at nodes internal to coarse blocks. However, the pressure equation solved on coarse cell edges is modified to include a cross-derivative term for pressure (a second derivative involving both x and y) — a form of diffusion. This analysis allows us to simplify the algorithmic implementation of the method and to gain an understanding of what the solution produced by this technique models physically.

Acknowledgments. We thank Alan Levander and Bill Symes of Rice University for asking the extremely pertinent question, "What does the upscaled solution mean?" We further thank Bill Symes for suggesting that we look at the upscaling algorithm as a linear algebra problem. His insight led to the work described in this

paper. We thank Tetyana Vdovina of UMBC for her help with the derivation of the continuous differential equations for pressure from the difference equations. Finally, we are grateful to John Zweck of UMBC for reading an early draft of the manuscript. His suggestions greatly improved the overall structure of the paper.

REFERENCES

[1] G. Allaire, *Homogenization and two-scale convergence*, SIAM J. Math. Anal., 23 (1992), pp. 1482–1518.
[2] T. Arbogast and K. Boyd, *Subgrid upscaling and mixed multiscale finite elements*, SIAM J. Numer. Anal., to appear.
[3] T. Arbogast and S. Bryant, *A two-scale numerical subgrid technique for waterflood simulations*, SPE J., 27 (2002), pp. 446–457.
[4] T. Arbogast, S. Minkoff, and P. Keenan, *An operator-based approach to upscaling the pressure equation*, Comput. Methods in Water Resources XII, 1 (1998), pp. 405–412.
[5] T. Arbogast, *Numerical Subgrid Upscaling of Two-Phase Flow in Porous Media*, Lect. Notes Phys. 552, Springer, Berlin, 2000.
[6] T. Arbogast, *Implementation of a locally conservative numerical subgrid upscaling scheme for two-phase flow*, Comput. Geosci., 6 (2002), pp. 453–48.
[7] A. Bensoussan, J. Lions, and G. Papanicolaou, *Asymptotic Analysis for Periodic Structure*, North-Holland, Amsterdam, 1979.
[8] D. Bergman, J. Lions, G. Papanicolaou, F. Murat, L. Tartar, and E. Sanchez-Palencia, *Les Méthodes de L'homogénéisation: Théorie et Applications en Physique*, Editions Eyrolles, Paris, 1985.
[9] Z. Chen and T. Hou, *A mixed multiscale finite element method for elliptic problems with oscillating coefficients*, Math. Comp., 72 (2002), pp. 541–576.
[10] M. Christie, *Upscaling for reservoir simulation*, J. Pet. Tech., 48 (1996), pp. 1004–1010.
[11] G. Cohen, *Higher-Order Numerical Methods for Transient Wave Equations*, Springer-Verlag, New York, 2002.
[12] T. Y. Hou, X. H. Wu, and Z. Cai, *Convergence of a multiscale finite element method for elliptic problems with rapidly oscillating coefficients*, Math. Comp., 68 (1999), pp. 913–943.
[13] T. Y. Hou, X. H. Wu, and Y. Zhang, *Removing the cell resonance error in the multiscale finite element method via a petrov-galerkin formulation*, Commun. Math. Science, 2 (2004), pp. 185–205.
[14] T. Hou and X. Wu, *A multiscale finite element method for elliptic problems in composite materials and porous media*, J. Comput. Phys., 134 (1997), pp. 169–189.
[15] M. Peszynska, M. Wheeler, and I. Yotov, *Mortar upscaling for multiphase flow in multiblock domains*, Comput. Geosci., 6 (2002), pp. 315–332.
[16] P. Renard and G. de Marsily, *Calculating equivalent permeability: A review*, Adv. in Water Resources, 20 (1997), pp. 253–278.
[17] T. Vdovina, S. Minkoff, and O. Korostyshevskaya, *Operator upscaling for the acoustic wave equation*, SIAM J. Multiscale Model. Simul., 4 (2005), pp. 1305–1338.
[18] X. Wu, Y. Efendiev, and T. Hou, *Analysis of upscaling absolute permeability*, Discrete Contin. Dyn. Syst., 2 (2002), pp. 185–204.
[19] I. Yotov, *Mortar mixed finite element methods on irregular multiblock domains*, in Iterative Methods in Scientific Computation, IMACS Ser. Comp. Appl. Math. 4, J. Wang, M. B. Allen, B. Chen, and T. Mathew, eds., International Association for Mathematics and Computers in Simulation, Brussels 1998, pp. 239–244.